

Joint profiling of DNA methylation and chromatin architecture in single cells

Guoqiang Li^{1,9}, Yaping Liu^{2,3,4,9}, Yanxiao Zhang¹, Naoki Kubo¹, Miao Yu¹, Rongxin Fang^{1,5}, Manolis Kellis^{6,7} and Bing Ren^{1,8*}

We report a molecular assay, Methyl-HiC, that can simultaneously capture the chromosome conformation and DNA methylome in a cell. Methyl-HiC reveals coordinated DNA methylation status between distal genomic segments that are in spatial proximity in the nucleus, and delineates heterogeneity of both the chromatin architecture and DNA methylome in a mixed population. It enables simultaneous characterization of cell-type-specific chromatin organization and epigenome in complex tissues.

DNA methylation is dynamically regulated^{1–3} and exhibits characteristic patterns in different cell types⁴. DNA methylation can be profiled by whole-genome bisulfite sequencing (WGBS) at base resolution⁵, which shows that the methylation status of adjacent CpGs is often correlated^{6,7}. Since DNA is spatially organized into three-dimensional structures, distal genomic regions may be brought into proximity through chromatin folding⁸. Thus, it is possible that spatially proximal DNA sequences may also exhibit coordinated DNA methylation. However, conventional WGBS has limited power to detect coordinated DNA methylation across large genomic distances due to short DNA fragments profiled in such assays.

The chromosome conformation capture technologies capture spatial proximity through restriction digestion and in situ ligation of proximal DNA segments^{9–12}. In principle, methylation status of cytosines on the ligated DNA is preserved in chromosome conformation capture experiments and can be detected through bisulfite sequencing approaches. We therefore developed Methyl-HiC, a method that combines in situ Hi-C¹¹ and WGBS⁵ to simultaneously profile chromatin conformation and DNA methylation. It begins with a standard in situ Hi-C procedure, followed by an additional step of bisulfite conversion before library construction and paired-end sequencing (Supplementary Fig. 1a). The methylation status of cytosines and the pair-wise contact frequencies are then determined using custom software (Supplementary Fig. 1b–e) (see Methods for description).

We applied Methyl-HiC to mouse embryonic stem cells (mESCs) (Supplementary Fig. 1f) and observed a contact matrix highly similar to that of in situ Hi-C (Fig. 1a), with indistinguishable distribution of contact probabilities as a function of genomic distances (Fig. 1b). Similar sets of chromatin loops were detected from both assays (Fig. 1a, Supplementary Fig. 2a,b and Supplementary Table 1). Comparable topologically associating domains (TADs) were also identified from the two datasets (Fig. 1c and Supplementary Fig. 2c,d). Comparing Methyl-HiC results with WGBS data from

the same cell type, Methyl-HiC data captured over 16 million CpGs in the mouse genome and the methylation levels of these CpGs were highly consistent with that from WGBS (Supplementary Fig. 2e and Fig. 1d). Notably, compared with WGBS, Methyl-HiC profiled about 20% fewer CpGs overall but relatively more CpGs in open chromatin regions such as promoters and enhancers, likely due to reduced access to heterochromatin by the restriction enzyme used in the procedure (Supplementary Fig. 2e,f). These results, taken together, demonstrate that Methyl-HiC can simultaneously and accurately profile both the general features of chromosomal architecture and >80% of the methylome in a biological sample.

Methyl-HiC allows us to test the hypothesis that cytosines linearly separated but positioned proximally in space may also have coordinated methylation status. We analyzed the CpG methylation on Methyl-HiC reads separated in chromatin loop anchors (Supplementary Fig. 3a–c). Indeed, the methylation status of CpGs in Methyl-HiC read pairs mapping to separated loop anchors showed a notable correlation (Fig. 1e and Supplementary Fig. 3d). Further, such correlation was not restricted to chromatin loops mediated by CTCF¹³, as loop anchors not occupied by CTCF also showed substantial correlation of DNA methylation (Supplementary Fig. 3e). We further tested whether chromatin organizational features influence such coordinated methylation. Indeed, Methyl-HiC read pairs within the same TADs exhibited slightly higher DNA methylation concordance than those from two different TADs (Supplementary Fig. 3f). Although read pairs in either compartment A or B showed similar DNA methylation concordance (Supplementary Fig. 3g), CpGs from loop anchors showed higher methylation concordance in compartment A than those in compartment B (Fig. 1f). We also observed a weaker but obvious concordance for inter-chromosomal interactions (Supplementary Fig. 3h). Finally, we observed that the degree of DNA methylation concordance varies depending on the underlying chromatin states (Supplementary Fig. 4).

To further demonstrate the utility of Methyl-HiC, we used it to analyze chromatin conformation and DNA methylation together in single cells. Cellular heterogeneity presents a significant challenge for chromatin architecture analysis in complex tissues^{4,14}. Single-cell Hi-C has previously been performed to characterize dynamic chromatin organization in early embryogenesis and during cell cycle^{15,16}, and to uncover the heterogeneity of chromatin architecture within a population of cells¹⁷. Single-cell Methyl-HiC (scMethyl-HiC) can in principle resolve the heterogeneity of both DNA methylation and chromatin organization from the same cells. To achieve this, we adapted the above

¹Ludwig Institute for Cancer Research, La Jolla, CA, USA. ²Division of Human Genetics, Cincinnati Children's Hospital Medical Center, Cincinnati, OH, USA. ³Department of Pediatrics, University of Cincinnati College of Medicine, Cincinnati, OH, USA. ⁴Cincinnati Cancer Center, University of Cincinnati, Cincinnati, OH, USA. ⁵Bioinformatics and Systems Biology Graduate Program, University of California, San Diego, La Jolla, CA, USA. ⁶Broad Institute of MIT and Harvard, Cambridge, MA, USA. ⁷Massachusetts Institute of Technology, Computer Science and Artificial Intelligence Laboratory, Cambridge, MA, USA. ⁸Department of Cellular and Molecular Medicine, Center for Epigenomics, Institute of Genomic Medicine, Moores Cancer Center, University of California, San Diego, School of Medicine, La Jolla, CA, USA. ⁹These authors contributed equally: Guoqiang Li, Yaping Liu. *e-mail: biren@ucsd.edu

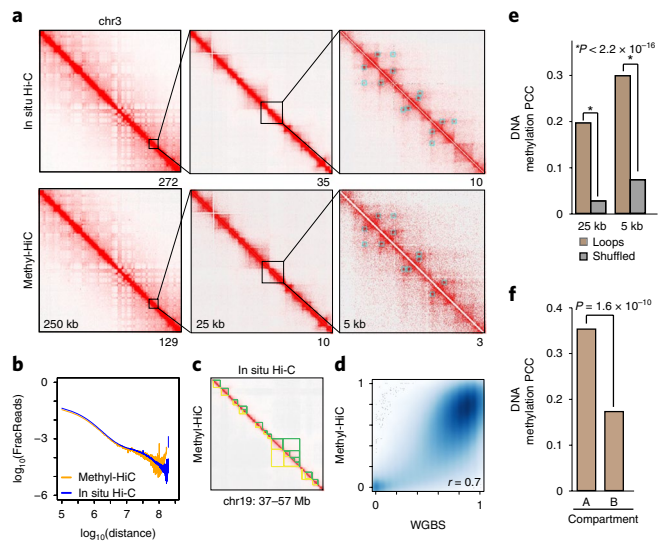


Fig. 1 | Methyl-HiC simultaneously profiles long-range chromatin

interactions and DNA methylome in mESCs. a, Comparison of contact matrix between in situ Hi-C and Methyl-HiC at different resolutions. Blue squares are loops identified from corresponding dataset at 25-kb resolution. Numbers below each map show the maximum contact values. **b**, Comparison of contact frequency distance decay curve obtained from in situ Hi-C and Methyl-HiC data. **c**, A snapshot on chromosome 19 showing TADs identified from in situ Hi-C and Methyl-HiC (yellow and green triangles, respectively). **d**, Scatter plot showing the Pearson correlation of DNA methylation in common CpGs with 15X coverage ($n=1,161,200$) between WGBS and Methyl-HiC datasets ($P < 2.2 \times 10^{-16}$) between WGBS and Methyl-HiC datasets ($P < 2.2 \times 10^{-16}$). **e**, Pearson correlation coefficient (PCC) of DNA methylation between chromatin loop anchors identified using HiCCUPS¹¹ at 5 kb and 25 kb resolutions. Only reads containing 2 or more CpGs on each end were included ($n=13,645$ for 5 kb and $n=53,645$ for 25 kb). Paired-end reads located within the same loop anchors were re-shuffled and used to calculate the expected values. Significance was assessed using Fisher's (1925) z in `cocor.indep.groups` function in `cocor` package in R²¹. **f**, PCC of DNA methylation on reads from loop anchors in compartment A ($n=14,016$) compared with those in compartment B ($n=12,126$). Significance was assessed using Fisher's (1925) z in `cocor.indep.groups` function in `cocor` package in R.

Methyl-HiC protocol for single-cell analysis. Briefly, after proximity ligation we sorted individual nuclei into 96-well plates where bisulfite conversion was carried out with each nucleus. The resulting DNA was then amplified for sequencing. We generated scMethyl-HiC data for 103 mESCs cultured in serum + leukemia inhibitory factor (LIF) condition (serum mESCs) and 47 mESCs cultured in LIF with GSK3 and MEK inhibitors (2i) condition (2i mESCs), obtaining a median number of 80,763 informative contacts per nucleus for serum mESCs and 64,618 for 2i mESCs (Supplementary Table 2). The contact probabilities of the aggregate scMethyl-HiC were comparable to the bulk dataset (Fig. 2a and Supplementary Fig. 5a–c), and to previously published single-cell Hi-C data of mESCs¹⁵ (Fig. 2b). The scMethyl-HiC experiments also generated DNA methylomes with an average of 567,380 CpGs per nucleus, comparable to previous single-cell methylome datasets^{4,18} (Supplementary Table 2). The average methylation levels of CpGs in serum and 2i mESCs were 61.9% and 23.4%, while the methylation levels of CpGs were 1.3% and 0.9% (Fig. 2c and Supplementary Table 2), respectively, which are also consistent with previous observations¹⁸. As in bulk Methyl-HiC data, DNA methylation at the chromatin loop anchors was coordinated in individual cells (Fig. 2d). These results showed that Methyl-HiC can simultaneously profile DNA methylation and chromatin architecture in single cells.

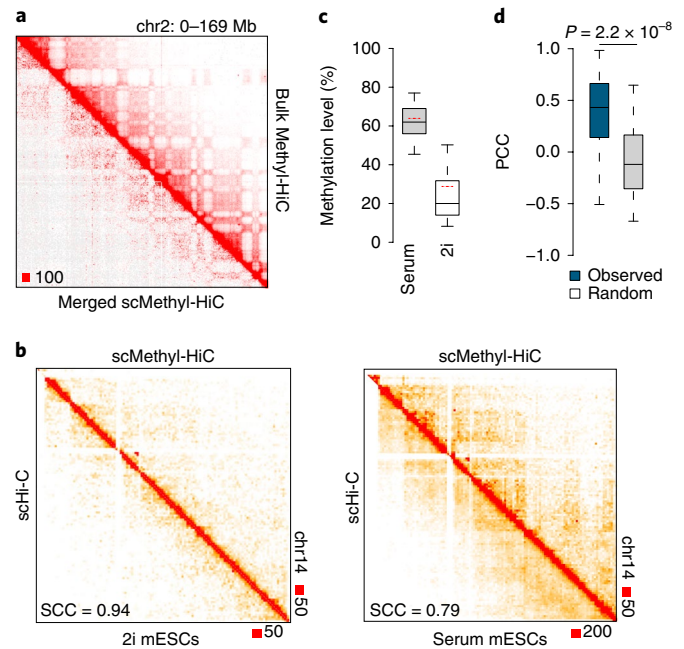


Fig. 2 | Simultaneous analysis of DNA methylome and chromatin

architecture in individual cells by scMethyl-HiC. a, Comparison between ensemble contact matrix of scMethyl-HiC from 103 serum mESCs and bulk Methyl-HiC on chromosome 2. Contact matrixes are normalized by sequencing coverage and showed at 1-Mb resolution. **b**, Comparison of contact matrixes on chromosome 14 between the same number ($n=50$) of ensemble single-cell Hi-C (scHi-C)¹⁵ and scMethyl-HiC for mESCs in 2i and serum conditions. Matrix similarity is evaluated by HiCRep²² at 1-Mb resolution. SCC, stratum-adjusted correlation coefficient. **c**, The comparison of methylation level distribution between serum ($n=103$) and 2i ($n=47$) mESCs from scMethyl-HiC. Boxes are median with quartiles and whiskers extend to 5th and 95th percentiles. Red dotted lines show the average methylation levels from previously published data¹⁸. **d**, DNA methylation concordance on loop anchors in individual scMethyl-HiC datasets. Chromatin loops are identified from bulk Methyl-HiC using HiCCUPS ($n=3,110$). Boxes are median with quartiles and whiskers extend to 5th and 95th percentiles.

To reveal the heterogeneity of the cell population using the above scMethyl-HiC data, we first clustered all of the cells based on the DNA methylome of each cell alone. Interestingly, in addition to a clear separation between mESCs grown in serum and 2i conditions, the mESCs grown in serum condition were further divided into two subpopulations, consistent with a previous report¹⁸ (Fig. 3a). We compared these subpopulations with DNA methylation profiles from multiple cell lineages and found that cluster 3 showed a potential embryonic limb development trend (Fig. 3b). The aggregate chromatin contact matrixes in each cluster also showed clear cluster-specific chromosome conformation (Fig. 3c), evidenced by differential compartments between clusters (Supplementary Fig. 6a and Supplementary Table 3) that were accompanied by differentially methylated regions (DMRs) (Supplementary Fig. 6b–d). Similarly, DMRs and genes located in these differential compartments were enriched with gene ontology terms related to embryonic limb development (Fig. 3d,e). For example, *Epha4* and genes within the *HoxD* locus¹⁹ were differentially methylated and exhibited differential compartments between cluster 2 and cluster 3 (Fig. 3f and Supplementary Fig. 6e,f). These results suggest that scMethyl-HiC can be used to resolve cell-type-specific chromosomal architecture in heterogeneous cell populations.

We propose that scMethyl-HiC may be used to study cell-type-specific epigenome and chromatin organization in complex tissues.

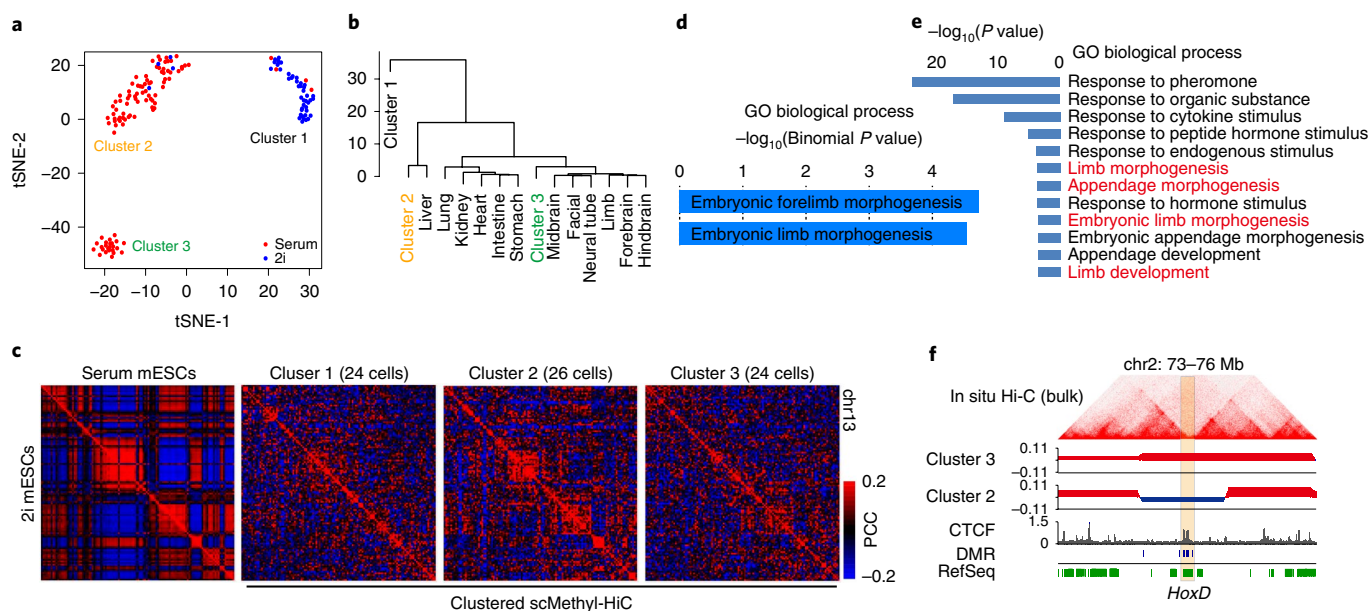


Fig. 3 | scMethyl-HiC reveals heterogeneity of cultured mESCs. **a**, tSNE visualization of unsupervised clustering results according to DNA methylation from individual scMethyl-HiC dataset ($n=150$). Methylation level is calculated in non-overlapping 1-Mb bins. **b**, Unsupervised clustering of aggregated DNA methylome in subgroups of serum mESCs with tissue-specific methylomes in mouse embryonic development. **c**, Pearson's correlation matrixes from different cell clusters. Similar numbers of cells are randomly selected to plot the matrixes ($n=24, 26$ and 24). The left map shows the bulk in situ Hi-C matrixes from serum and 2i mESCs, respectively. Pearson's correlation coefficient is calculated under 1-Mb resolution. Color ranges have been set to the same scale. **d**, GO biological process terms predicted by GREAT (genomic regions enrichment of annotations tool) for DMRs ($n=99$) switching from compartment B in cluster 2 to compartment A in cluster 3. **e**, GO biological process terms of genes ($n=672$) switching from compartment B in cluster 2 to compartment A in cluster 3. P values are from modified Fisher exact test for gene-enrichment analysis. **f**, Snapshot of *HoxD* cluster genes in differential compartments between clusters 2 and 3. Hi-C matrixes are from bulk in situ Hi-C of the same cell line to show the chromosome organization in nearby regions. The two tracks below the Hi-C matrix are the eigenvector decomposition. The positive/negative values correspond to compartment A/B, respectively. DMRs between cluster 2 and cluster 3 are also plotted. GO, gene ontology; tSNE, t-distributed stochastic neighbor embedding.

While the current scMethyl-HiC protocol is still limited by data sparsity, this limitation may be overcome in the future by alternative DNA methylation detection strategies²⁰.

Online content

Any methods, additional references, Nature Research reporting summaries, source data, statements of code and data availability and associated accession codes are available at <https://doi.org/10.1038/s41592-019-0502-z>.

Received: 14 November 2018; Accepted: 24 June 2019;
Published online: 5 August 2019

References

- Iurlaro, M., von Meyenn, F. & Reik, W. *Curr. Opin. Genet. Dev.* **43**, 101–109 (2017).
- Lyko, F. *Nat. Rev. Genet.* **19**, 81–92 (2018).
- Guo, J. U., Su, Y., Zhong, C., Ming, G.-I. & Song, H. *Cell* **145**, 423–434 (2011).
- Luo, C. et al. *Science* **357**, 600 (2017).
- Lister, R. et al. *Nature* **462**, 315 (2009).
- Guo, S. et al. *Nat. Genet.* **49**, 635 (2017).
- Shoemaker, R., Deng, J., Wang, W. & Zhang, K. *Genome Res.* **20**, 883–889 (2010).
- Dixon, JesseR., Gorkin, DavidU. & Ren, B. *Mol. Cell* **62**, 668–680 (2016).
- Lieberman-Aiden, E. et al. *Science* **326**, 289 (2009).
- Dixon, J. R. et al. *Nature* **485**, 376 (2012).
- Rao, SuhasS. P. et al. *Cell* **159**, 1665–1680 (2014).
- Schmitt, A. D., Hu, M. & Ren, B. *Nat. Rev. Mol. Cell Biol.* **17**, 743 (2016).
- Kubo, N. et al. Preprint at *bioRxiv* <https://doi.org/10.1101/118737> (2017).
- Schwartzman, O. & Tanay, A. *Nat. Rev. Genet.* **16**, 716 (2015).
- Nagano, T. et al. *Nature* **547**, 61–67 (2017).
- Flyamer, I. M. et al. *Nature* **544**, 110 (2017).
- Ramani, V. et al. *Nat. Methods* **14**, 263–266 (2017).

- Smallwood, S. A. et al. *Nat. Methods* **11**, 817 (2014).
- Rodríguez-Carballo, E. et al. *Genes Dev.* **31**, 2264–2281 (2017).
- Liu, Y. et al. *Nat. Biotechnol.* **37**, 424–429 (2019).
- Diedenhofen, B. & Musch, J. *PLoS ONE* **10**, e0121945 (2015).
- Yang, T. et al. *Genome Res.* **27**, 1939–1949 (2017).

Acknowledgements

We thank S. Kuan and B. Li for processing of sequencing. The study was supported in part by the NIH 4D Nucleome program (grant no. U54DK107977) (to B.R.), grant no. 1U01HG007610-01 (to M.K.) and a start-up grant from CCHMC (to Y.L.).

Author contributions

B.R., G.L. and Y.L. conceived the study and prepared the manuscript. G.L. performed the Methyl-HiC experiments. Y.L. wrote the bioinformatics pipeline and performed the analysis with the guidance of M.K. Y.L., G.L. and Y.Z. performed the in situ Hi-C and WGBS analyses. M.Y. and R.F. helped on single-cell Hi-C data analysis. N.K. provided the list of loops with CTCF. G.L., Y.L. and B.R. wrote the manuscript.

Competing interests

B.R. is a cofounder of Arima Genomics, Inc.

Additional information

Supplementary information is available for this paper at <https://doi.org/10.1038/s41592-019-0502-z>.

Reprints and permissions information is available at www.nature.com/reprints.

Correspondence and requests for materials should be addressed to B.R.

Peer review information: Nicole Rusk was the primary editor on this article and managed its editorial process and peer review in collaboration with the rest of the editorial team.

Publisher's note: Springer Nature remains neutral with regard to jurisdictional claims in published maps and institutional affiliations.

© The Author(s), under exclusive licence to Springer Nature America, Inc. 2019

Methods

Cell culture. The F1 *Mus musculus castaneus* × S129/SvJae mouse embryonic stem cell line (F123) was obtained from Whitehead Institute as described previously²³. Serum mESCs were cultured with irradiated mouse embryonic fibroblasts (Gibco, A34180) in medium with 85% DMEM, 15% Knock-out Serum Replacement (Gibco, 10828-028), 1X penicillin/streptomycin, 1X non-essential amino acids (Gibco, 11140-050), 1X GlutaMax (Gibco, 35050), 0.4 mM β-mercaptoethanol and 1,000 U ml⁻¹ LIF (Millipore, ESG1107). 2i mESCs were adapted from serum mESCs by passing cells in MEF (mouse embryonic fibroblast) and serum-free 2i medium, which contained 50% Neurobasal (Gibco, 21103-049), 50% DMEM/F12 (Gibco, 11320-033), 0.5% N-2 Supplement (Gibco, 17502-048), 1% B27+RA (Gibco, 17504-044), 0.05% BSA (Gibco, 15260-037), 1X penicillin/streptomycin, 2 mM glutamine (Gibco, 25030-081), 150 μM monothioglycerol (Sigma, M6145), 1,000 U ml⁻¹ LIF (Millipore, ESG1107), 1 μM MEK inhibitor (Stemgent, 04-0006) and 3 μM GSK3 inhibitor (Stemgent, 04-0004). Serum mESCs were collected and plated on 0.2% gelatin-coated feeder-free plates for 30 min before collecting to remove feeder cell contamination.

Methyl-HiC. In situ Hi-C was performed according to a published protocol¹¹. Briefly, 2 million cells were cross-linked with 1% formaldehyde for 10 min at room temperature. Reaction was then quenched with 0.2 M Glycine. Cell pellets were washed with cold PBS and lysed with lysis buffer to get nuclei pellets. Nuclei were permeabilized with 0.5% SDS. DNA was in situ digested with 100 units of DpnII (NEB, R0543) overnight. The ends of restriction fragments were filled with biotinylated nucleotides (Invitrogen, 19524016) and in situ ligated with T4 DNA ligase (NEB, M0202). After reversal of cross-links, ligated DNA was ethanol precipitated and sheared to about 400 base pairs (bp) by sonication (Covaris). Sonicated products were pulled down with streptavidin beads. Library construction was then performed on beads. After adapter ligation, beads were suspended in 20 μl TE buffer and subjected to bisulfite conversion with EZ DNA Methylation-Gold Kit (Zymo, D5005). Unmethylated lambda DNA (Promega, D1501) was sonicated and ligated with the same adapter for the Methyl-HiC sample and then was spiked in at 0.5% before bisulfite conversion. Purified bisulfite-converted DNA was amplified with HiFi Hotstart Uracil+Ready Mix (KAPA, KK2802).

scMethyl-HiC. In situ Hi-C was performed the same as above for bulk Methyl-HiC up to the steps of proximal ligation. After ligation, nuclei pellets were centrifuged and washed with PBS. Pellets were suspended in PBS stained with 1:200 DRAQ7 (CST, 7406S). The nuclei were FACS sorted, 1 nucleus at a time, into a 96-well plate containing 9 μl PBS in each well. Bisulfite conversion was then performed in each well with EZ-96 DNA Methylation-Direct Kit according to the manufacturer's manual (Zymo, D5020). Fragmented lambda DNA (0.5%) was spiked in before bisulfite conversion. Following bisulfite conversion of single nuclei, random priming of bisulfite-converted DNA with high-concentration Klenow fragments (Enzymatics, P706L) incorporated an internal indexed P5 adapter to 5' ends of synthesized fragments, which could be used for downstream multiplexing capability. Exonuclease I (NEB, M0293) and Shrimp Alkaline Phosphatase (NEB, M0371) treatments were then performed to digest unused random primer and inactivate dNTPs, followed by an SPRI bead-based purification step. P7 adapters were then ligated to the 3' end of single-stranded products by Adaptase module (Swift, 33096). Library amplification was then performed using indexed primers that incorporate dual indexing to enable 96-plex sequencing. Amplified libraries were pooled together and subjected to size selection and library quantification. Please refer to the Supplementary protocol for more details.

WGBS. Genomic DNA was first extracted from mESCs (Qiagen, 69504). Genomic DNA (1–1.5 μg) was fragmented by sonication (Covaris), end-repaired, dA-tailed and ligated to cytosine-methylated Illumina Truseq adapter. Ligation product was subjected to bisulfite conversion reaction according to the manufacturer's instructions (Zymo, D5005). Unmethylated λDNA (0.5%) was spiked in before the conversion. Bisulfite-converted DNA was then PCR amplified and purified.

Sequencing of DNA libraries. The quantification of sequencing libraries was determined by quantitative PCR and TapeStation DNA analyzer (Agilent Technologies). Pooling of multiplexed sequencing samples, clustering and sequencing were carried out as recommended by the manufacturer on an Illumina HiSeq 2500 or HiSeq 4000. For bisulfite-converted libraries, at least 50% of balanced libraries or Phix were multiplexed to overcome the imbalance of GC ratio. All libraries were sequenced in paired-end mode.

Analysis of WGBS data. Raw reads were first trimmed as paired-end reads using Trimmomatic with default parameters to remove the adapters and low-quality reads. Trimmomatic reads were aligned to mm9 using Bismark (v.12.5). PCR duplications were removed with Picard (<http://broadinstitute.github.io/picard/>). CpG methylation levels were calculated by Bis-SNP in bisnp_easy_usage.pl with default parameters.

Analysis of in situ Hi-C data. Each end of the raw reads was mapped separately to the mm9 reference genome using BWA-mem. Filtered reads were then paired with in-house script and de-duplicated by Picard. Reads that mapped to the same fragment were further removed. Contact matrices were generated at different resolutions using Juicer pipeline with KR (Knight and Ruiz) normalization and visualized using Juicebox²⁴. Loops were then called by HiCCUPS¹.

Methyl-HiC read mapping by Bhmeme. Raw reads were first trimmed as paired-end reads using Trimmomatic with default parameters to remove the adapters and low-quality reads. The reference genome was in silico converted to make C/T reference (all Cs were converted to Ts) and G/A reference (all Gs were converted to As). Paired-end reads were mapped in single-end mode to each converted reference by BWA-MEM. Only uniquely mapped and mapping quality-passed reads on both ends were joined. Joint read pairs with more than 20 kb insertion size were considered as long-range interactions and subjected to the following interaction analysis. CpG methylation levels were calculated by Bis-SNP²⁵. Only bases with quality score more than 5 were included in the downstream methylation analysis. More details were implemented in Bhmeme.java.

Correlation analysis of methylation in Methyl-HiC datasets. The reads with large fraction of incompletely converted cytosines were filtered out as previously described²⁵. Only read pairs with methylation levels at both ends were kept for the analysis. For the regions of interests, such as HiCCUPS loops anchor regions, Pearson correlation coefficient (PCC) was calculated directly from the methylation level of each read of the read pair, not by the average methylation level at each end of anchor regions. Only read pairs spanning at least 20 kb genomic distance were considered for the analysis. As control, all of the read pairs within the same genomic region no matter whether they had long-range interaction or not were randomly shuffled 100 times and then subjected to PCC calculation. Fisher's (1925) z, implemented in 'cocor.indep.groups' in R package 'cocor'²¹, was used to assess the significance between the observed PCC from interacted read pairs and the PCC of random read pairs. The scripts for this analysis are provided in MethylCorAcrossHiCCups.java.

scMethyl-HiC analysis. Reads were mapped by the same Bhmeme pipeline with additional parameters to adapt the single-cell protocol (G was converted to A in read 1 and C was converted to T in read 2; read 1 and read 2 mapped to different bisulfite-converted genomes were also considered as candidates for selecting best pair when join them). For read pairs uniquely mapped to different locations of C/T reference and G/A reference, we first filtered out those with lower mapping quality and higher mismatch number. For these multiple-mapped read pairs with exact mapping quality and mismatches, we then utilized the restriction enzyme cutting sites on the reference genome to help with the read mapping. Only read pairs with restriction enzyme cutting sites near the reads (±50 bp from alignment start and end of the reads) were kept for further analysis. Low-quality reads, PCR duplicates and read ends originating from the same location but with more than ten distinct paired ends were removed for further analysis. Reads originating from distinct restriction fragments and with linear distance larger than 1 kb in *cis* were considered as informative contacts. Contact matrices were generated at different resolutions using Juicer pipeline with VC (vanilla coverage) normalization and visualized using Juicebox²⁴. Ensemble matrix similarity was evaluated by HiCRep²².

Methylation densities on CpGs and CpHs were calculated with Bis-SNP. The methylation level in each non-overlapped 1-Mb window was further calculated and bins with missing data were replaced by the mean methylation level of bins at the same location across all single cells. Bins with missing data in all of the cells were removed from analysis. Then, t-distributed stochastic neighbor embedding was applied to represent the methylation level structure at the single-cell level (Rtsne package in R version 3.4.0 with plexity = 10 and max_iter = 5,000). Different plexity level and random seed were applied to test the robustness of representation. Methylated count and total count (missing data are not replaced by mean value yet) at each window within each subcluster were aggregated, and then the methylation level was calculated. DNA methylomes of different development lineages were from ENCODE. Methylation density was also calculated in non-overlapped 1-Mb windows. Euclidean distances between three merged scMethyl-HiC clusters and external ENCODE methylomes were calculated and clustered by 'ward.D2' implemented in hclust function in R.

Reporting Summary. Further information on research design is available in the Nature Research Reporting Summary linked to this article.

Data availability

Figures show merged data from all replicates. The bulk Methyl-HiC, single-cell Methyl-HiC and WGBS datasets generated in this study have been deposited in the Gene Expression Omnibus (GEO) under the accession number GSE119171. Previously published data used for this study are listed in the Supplementary Notes.

Code availability

All of the source code for Bhmeme software is publicly available at Bitbucket via <https://bitbucket.org/dnaase/bisulfitehic/src/master/>

References

- Gribnau, J., Hochedlinger, K., Hata, K., Li, E. & Jaenisch, R. *Genes Dev.* **17**, 759–773 (2003).
- Durand, N. C. et al. *Cell Syst.* **3**, 99–101 (2016).
- Liu, Y., Siegmund, K. D., Laird, P. W. & Berman, B. P. *Genome Biol.* **13**, R61 (2012).

Reporting Summary

Nature Research wishes to improve the reproducibility of the work that we publish. This form provides structure for consistency and transparency in reporting. For further information on Nature Research policies, see [Authors & Referees](#) and the [Editorial Policy Checklist](#).

Statistical parameters

When statistical analyses are reported, confirm that the following items are present in the relevant location (e.g. figure legend, table legend, main text, or Methods section).

n/a Confirmed

- The exact sample size (n) for each experimental group/condition, given as a discrete number and unit of measurement
- An indication of whether measurements were taken from distinct samples or whether the same sample was measured repeatedly
- The statistical test(s) used AND whether they are one- or two-sided
Only common tests should be described solely by name; describe more complex techniques in the Methods section.
- A description of all covariates tested
- A description of any assumptions or corrections, such as tests of normality and adjustment for multiple comparisons
- A full description of the statistics including central tendency (e.g. means) or other basic estimates (e.g. regression coefficient) AND variation (e.g. standard deviation) or associated estimates of uncertainty (e.g. confidence intervals)
- For null hypothesis testing, the test statistic (e.g. F , t , r) with confidence intervals, effect sizes, degrees of freedom and P value noted
Give P values as exact values whenever suitable.
- For Bayesian analysis, information on the choice of priors and Markov chain Monte Carlo settings
- For hierarchical and complex designs, identification of the appropriate level for tests and full reporting of outcomes
- Estimates of effect sizes (e.g. Cohen's d , Pearson's r), indicating how they were calculated
- Clearly defined error bars
State explicitly what error bars represent (e.g. SD, SE, CI)

Our web collection on [statistics for biologists](#) may be useful.

Software and code

Policy information about [availability of computer code](#)

Data collection

No software was used for data collection.

Data analysis

Published software for data analysis used throughout the study includes BWA-MEM (bwa-0.7.12), FastQC v0.11.4, picard-tools-1.118, BisSNP-0.82.2.jar, bismark_v0.14.5, bedtools2-2.24.0,samtools-1.2, Trimmomatic-0.33, bedGraphToBigWig, juicer_tools.1.7.6, juicebox_tools.7.5, sambamba_v0.6.3, bamtools-2.4.0, and SNPsplit_v0.3.0. All the source code for Bhemem software is publicly available at Bitbucket via <https://bitbucket.org/dnaase/bisulfitehic/src/master/>.

For manuscripts utilizing custom algorithms or software that are central to the research but not yet described in published literature, software must be made available to editors/reviewers upon request. We strongly encourage code deposition in a community repository (e.g. GitHub). See the Nature Research [guidelines for submitting code & software](#) for further information.

Data

Policy information about [availability of data](#)

All manuscripts must include a [data availability statement](#). This statement should provide the following information, where applicable:

- Accession codes, unique identifiers, or web links for publicly available datasets
- A list of figures that have associated raw data
- A description of any restrictions on data availability

The Methyl-HiC, single cell Methyl-HiC, and WGBS data sets generated in this study have been deposited in the Gene Expression Omnibus (GEO) under the accession number GSE119171. Previously published data used for this study are listed in Supplementary Table 4.

Field-specific reporting

Please select the best fit for your research. If you are not sure, read the appropriate sections before making your selection.

Life sciences Behavioural & social sciences Ecological, evolutionary & environmental sciences

For a reference copy of the document with all sections, see [nature.com/authors/policies/ReportingSummary-flat.pdf](https://www.nature.com/authors/policies/ReportingSummary-flat.pdf)

Life sciences study design

All studies must disclose on these points even when the disclosure is negative.

Sample size	Sample sizes were chosen to provide sufficient confidence to validate methodological conclusions of the applicability of single cell Methyl-HiC.
Data exclusions	In the single cell Methyl-HiC datasets, after removing low quality reads (not unique mapped, PCR duplicate), cells with less than 250,000 reads and 10,000 contacts were removed for the further analysis. The rational behind this was that the limited reads number from individual cells cannot represent the chromatin and DNA methylation status very well. The exclusion criteria were not pre-established.
Replication	Bulk Methyl-HiC were performed with three replicates. We merged all the replications together for the further analysis. The reproducibility analysis for single cell Methyl-HiC is performed in Supplementary Fig. 5d. All attempts at replication were successful.
Randomization	Not relevant to this study as we didn't include experimental groups of samples/organism/participants.
Blinding	Not relevant to this study as we didn't include group allocation.

Reporting for specific materials, systems and methods

Materials & experimental systems

n/a	Involved in the study
<input checked="" type="checkbox"/>	<input type="checkbox"/> Unique biological materials
<input checked="" type="checkbox"/>	<input type="checkbox"/> Antibodies
<input type="checkbox"/>	<input checked="" type="checkbox"/> Eukaryotic cell lines
<input checked="" type="checkbox"/>	<input type="checkbox"/> Palaeontology
<input checked="" type="checkbox"/>	<input type="checkbox"/> Animals and other organisms
<input checked="" type="checkbox"/>	<input type="checkbox"/> Human research participants

Methods

n/a	Involved in the study
<input checked="" type="checkbox"/>	<input type="checkbox"/> ChIP-seq
<input type="checkbox"/>	<input checked="" type="checkbox"/> Flow cytometry
<input checked="" type="checkbox"/>	<input type="checkbox"/> MRI-based neuroimaging

Eukaryotic cell lines

Policy information about [cell lines](#)

Cell line source(s)	The F1 Mus musculus castaneus × S129/SvJae mouse ESC line (F123) was a gift from the Whitehead Institute. Mouse embryonic fibroblasts were purchased from Gibco (Gibco, A34180).
Authentication	Mouse embryonic fibroblasts were commercially available and authenticated by the manufacturer. F123 cell line was not authenticated to the best of our knowledge.
Mycoplasma contamination	Cell line was not tested for mycoplasma contamination in this project.

Commonly misidentified lines
(See [ICLAC](#) register)

No commonly misidentified cell lines were used.

Flow Cytometry

Plots

Confirm that:

- The axis labels state the marker and fluorochrome used (e.g. CD4-FITC).
- The axis scales are clearly visible. Include numbers along axes only for bottom left plot of group (a 'group' is an analysis of identical markers).
- All plots are contour plots with outliers or pseudocolor plots.
- A numerical value for number of cells or percentage (with statistics) is provided.

Methodology

Sample preparation

For single cell Methyl-HiC, In situ Hi-C was performed on F123 mESCs as same as above bulk Methyl-HiC till proximal ligation. After ligation, nuclei pellets were centrifuged and washed with PBS. Pellets were suspended in PBS stained with 1:200 DRAQ7 (CST, 7406S).

Instrument

Sony, SH800

Software

Sony, SH800 software

Cell population abundance

The percentage of nucleus collected was around 40%, which was determined by DRAQ7 staining.

Gating strategy

Positive and negative boundaries were determined by DRAQ7 staining, which specified the nucleus in interphase.

- Tick this box to confirm that a figure exemplifying the gating strategy is provided in the Supplementary Information.